Multi–Input Multi–Output Active Vibration Control for High Frequency Random Vibration

Aabhas Singh
University of Wisconsin – Madison
Singh36@wisc.edu

Matt Allen
University of Wisconsin - Madison
msallen@engr.wisc.edu

Washington J. DeLima
Honeywell[1]
Kansas City, MO, USA
wdelima@kcp.com

ABSTRACT

Electromagnetic shakers and closed loop control systems are commonly used in qualification tests for environmental vibration conditions. However, at high frequencies shakers have resonances and anti-resonances. Resonances can be beneficial in that the shaker needs to exert less force to achieve the desired environment, but they can make it more challenging for the control system to match the desired environment. Anti-resonances are more problematic because they represent frequencies where the voltage input to the shaker causes little motion (at some locations on the slip table or adapter plate). Hence, these can cause the system to require driver voltage levels above the controller capacity and cause the test to abort. Furthermore, an anti-resonance is in essence a motion that is unobserved at the point(s) of interest, and hence they may lead to damage if internal components experience much higher vibration levels than the control accelerometer. This paper proposes and characterizes a hybrid shaker system that would use a piezoelectric actuator in addition to the electromagnetic shaker to create a MIMO control system. It is hoped that the additional control effort introduced by the piezoelectric actuator could be used to expand the frequency range over which the desired environment can be achieved.

Keywords: Modal Test, model calibration

[1] Honeywell Federal Manufacturing & Technologies, LLC manages and operates the Department of Energy's Kansas City National Security Campus under contract DE-NA-0002839.

1. INTRODUCTION

Electromagnetic shakers are commonly used to replicate the motion of a test part under environmental vibration conditions. To do so, modern shakers must be capable of large displacements and high force levels and as a result, are large and have low frequency resonances, often hindering high frequency vibration tests. At higher frequencies above the first resonance of the shaker, uncontrollable modes of the shaker armature are excited, which can make it difficult or impossible to replicate the desired environment and which could result in damage to the shaker armature. These high-frequency modes can be highly variable between shakers, as shown recently by DeLima and Ambrose [1] , who measured the driver voltage necessary to achieve a desired environment for four shakers (UD-T2000®) as a function of the forcing frequency, a result that is repeated in Figure 1. As expected, at resonance there is a dip in the driver voltage, since the force required to excite the structure is minimized. However, at higher frequencies the behavior of the four shakers becomes erratic, deviating significantly from each other. In addition, at higher frequencies, the driver voltages peak, indicating anti-resonances or frequencies in which the test part moves little in response to the input force, so one must increase the voltage significantly to obtain the desired motion and the necessary voltage may be outside the capability of the shaker.

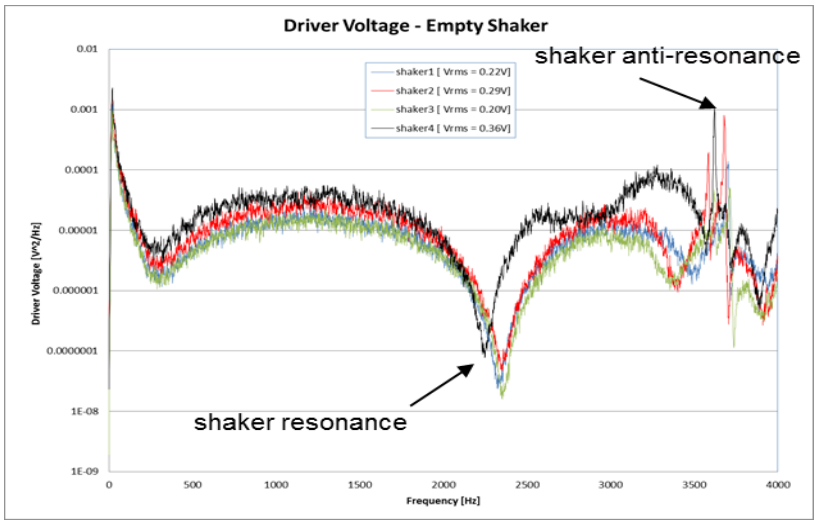

Figure 1: *Experimental Setup for the Shaker Test [1]*

This paper evaluates the potential to add piezoelectric actuators to a traditional electromagnetic shaker, so that a multi-input multi-output control scheme can be used to extend random test vibrations to higher frequencies without the potential of damaging the shaker structure. Past work to surpass these limitations of the shaker researched the sole use of piezo actuators to force test articles to a desired environment. This proved successful at high frequencies given that piezo actuators can support large-weight articles and render large forces [2]. However, the stroke length limitations of piezo actuators limit the displacement imposed on the test article. This work seeks to use MIMO control so that a traditional shaker and a piezo actuator can be used simultaneously, each working in the frequency range in which it is most effective, in hopes of reproducing the complete environment in a single test.

Prior to designing the control scheme, extensive modeling is required to understand the effects of coupling between the piezoelectric actuator and electrodynamic shaker motion. Piezoelectric actuators are somewhat fragile (made from brittle ceramic) so care must be taken to assure that the piezo actuator is not stressed beyond its limits. As a result, this work will validate three models for the piezo/shaker with varying degrees of fidelity to gauge their

effectiveness to provide the desired forces and survive the vibration environment: (1) a two degree of freedom model for the shaker, (2) a two degree of freedom model for the piezo actuator, and (3) a three degree of freedom model for the assembly.

The following sections discuss the tests that were used to characterize each of the components and the model calibrations done to equate to the test data.

2. EXPERIMENTAL CHACTERIZATION & MODELING OF SHAKER

The electrodynamic shaker and piezoelectric actuator system under investigation consists of a Brüel Kjær LDS V830-335 Metric Shaker coupled with the CEDRAT PPA40XL Actuator. Prior to creating the models, both components were characterized through modal analysis, and then the two models were assembled to evaluate the effectiveness of the coupled model. The modal test of the shaker was performed using 25 input points that followed the bolt pattern on the plate and two output points (accelerometers) as depicted in Figure 2.

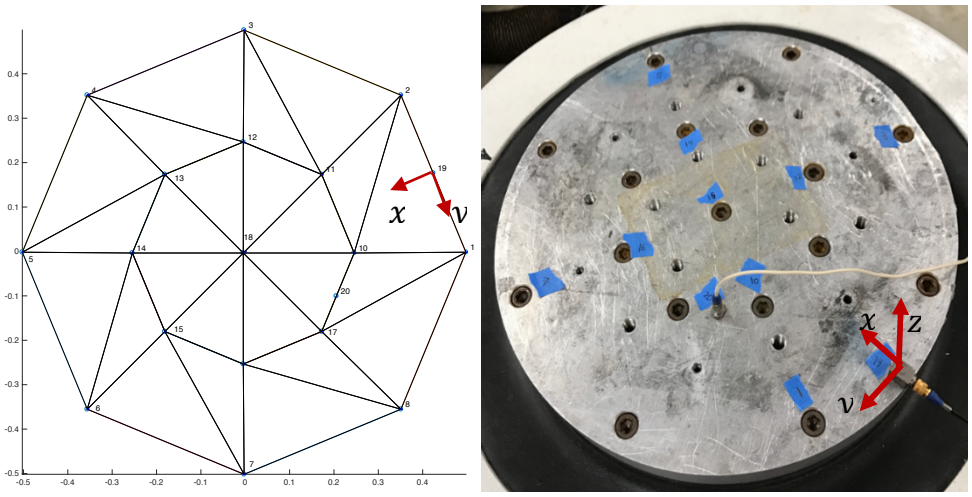

Figure 2: *Experimental Setup for the Shaker Test*

As with the experimental analysis done by DeLima, et.al [1], the frequency bandwidth was limited to approximately 4 kHz. Frequency Response Functions (FRFs) were measured for four DOF at two points on the plate: a triaxial accelerometer at point 19, and a uniaxial accelerometer (Z direction) at point 20. The mode shapes of the shaker and the plate are obtained using the FRFs with modal parameter identification using the Algorithm for Mode Isolation (AMI) [3], resulting in eight modes listed in Table 1.

Table 1: *Modes and the identified resonant frequencies and damping ratios*

Mode	Resonant Frequency (Hz)	Damping Ratio (%)	Mode Shape Description
1	1373	0.604	Y-axis rocking of top plate
2	2145.7	0.216	1st drum mode of top plate / assumed axial mode of shaker
3	2161.4	0.429	X-axis rocking of top plate with minor bending
4	2181	0.665	Y-axis rocking of top plate with minor bending

5	2627.5	1.30	1st torsion (“potato chip”) of top plate, 2 radial node lines
6	3290.5	1.09	1st drum mode of top plate, about center of mass
7	3845.5	0.782	2nd torsion of top plate, 3 radial node lines
8	4160	0.602	1st drum mode of top plate with edge distortion

The mode of primary interest is the first axial mode of the shaker, which was found to be at 2145.7 Hz and whose mode shape is shown below. Note that measurements were only taken on the shaker adapter plate, so it is impossible to characterize them separately with complete certainty. After the second mode, all of the modes involve zero motion of the center of the shaker plate until the 3290.5 Hz mode, suggesting that the 2DOF model of the shaker could be effective up until near that frequency.

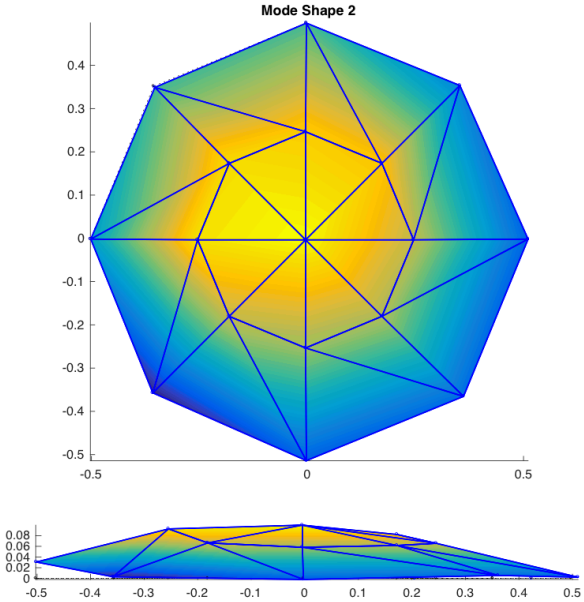

Figure 3: *Mode shape of Mode 2 at 2145.7 Hz*

2.1 2DOF ELECTRODYNAMIC SHAKER MODEL

The model for the electrodynamic shaker is based on the work by Waimer et al. [4]. The simplest model is a 2DOF lumped parameter model as shown in Figure 4. A two-mass system is the lowest order system that could exhibit the anti-resonances seen in the experiments by DeLima and Ambrose. Unlike Waimer, this model does not incorporate rotational shaker modes, given that the shaker is expected to be run at low frequencies, mitigating the non-axial modes.

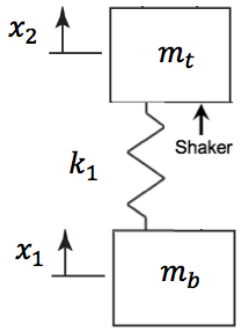

Figure 4: *2DOF model of the shaker armature*

A few parameters of the shaker are known from test and/or the manufacturer's specifications, and are noted in Table 2.

Table 2: *Notable LDS Shaker Parameters*

LDS V830-335 Shaker Parameters	
Armature Diameter	335 mm
Experimental Armature Resonance	2.146 kHz
Armature Mass	12.83 kg
Usable Frequency Range	0 – 3 khz

It is assumed that the system is lightly damped, with 0.2% modal damping for its axial mode. The natural frequency of the armature was measured and found to be approximately 2146 Hz. However, we do not have enough information to know how to divide the armature mass between the top plate and the internals of the shaker armature. Hence, in order to create this first model, the mass was simply divided such that 89% of the mass was placed on the top plate and 11% on the bottom in an effort to equate to experimental data. Then the stiffness was tuned such that the fundamental resonance frequency of the model matched the experimental resonance as shown in Table 3. Hence, the 2DOF system can be represented with the following parameters:

Table 3: *Shaker Model Parameters*

Upper Shaker Mass	11.41 kg
Lower Shaker Mass	1.42 kg
Armature Stiffness	3e8 N/m
Percent Damping	0.05%

In the interest of brevity, no measurements are shown to confirm this model, but it will be confirmed in conjunction with the piezo model in Section 4.

3. EXPERIMENTAL CHACTERIZATION & MODELING OF PIEZOELECTRIC ACTUATOR

A modal test of the piezo actuator was also performed, with one of the primary goals being to see what resonances it might have that could be excited in a test and hence could damage the piezo. As a first step, the CEDRAT piezo actuator was characterized in free-free conditions by laying the actuator on a foam pad. A modal hammer test was performed with 14 input points and a tri-axial accelerometer output at the top of the piezo, from which four modes were identified within the frequency range of interest; their properties are shown in Table 4.

Table 4: *Modes and the identified resonant frequencies and damping ratios*

Mode	Resonant Frequency (Hz)	Percent Damping
1	2562.5	0.302
2	2592	0.170
3	2727.1	1.117
4	2743.6	0.437

All four modes in this range correspond to bending of one of the four springs on the piezo, as seen with mode 2 below. The identified shapes suggest that these modes may be negligible if the motion is primarily axial, although this frequency range should be monitored to make sure that these lightly damped modes aren't excited. No other modes were observed in the frequency range of interest.

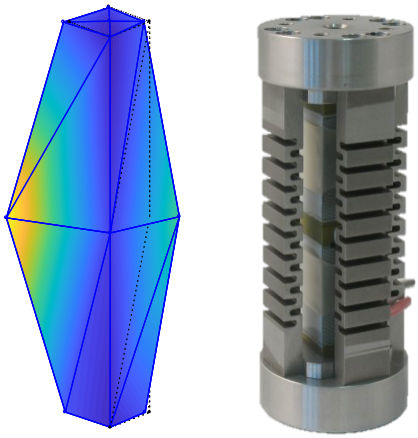

Figure 5: *2.59 kHz mode of the piezo*

In addition to modal tests done to understand the dynamics of the actuator in isolation, the piezo actuator was run at low input voltage with free – free conditions to model its ability to generate force. Free – blocked conditions were then added to validate the model predicted simulations. Lastly, the piezo actuator was bolted to the shaker using a fixture and each component was then excited separately to correlate to the coupled model as depicted in Figure 6.

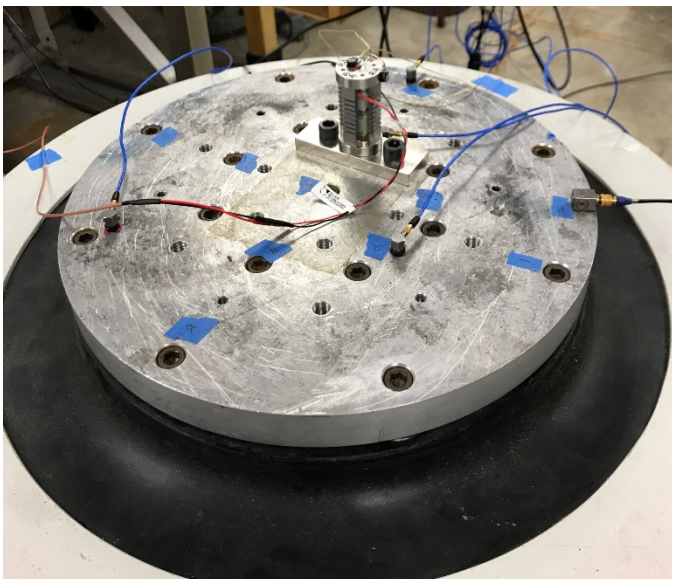

Figure 6: *Experimental setup used to test the piezo actuator on the shaker. Two other setups were also used that are not shown: 1) Bare piezo actuator mounted on foam, 2) Piezo actuator with a steel mass mounted to one end, mounted on foam.*

3.1 2DOF PIEZO ACTUATOR MODEL

The simplest model of the piezoelectric actuator is a 2DOF model, as discussed in the CEDRAT Catalog [5] and shown in Figure 7 below.

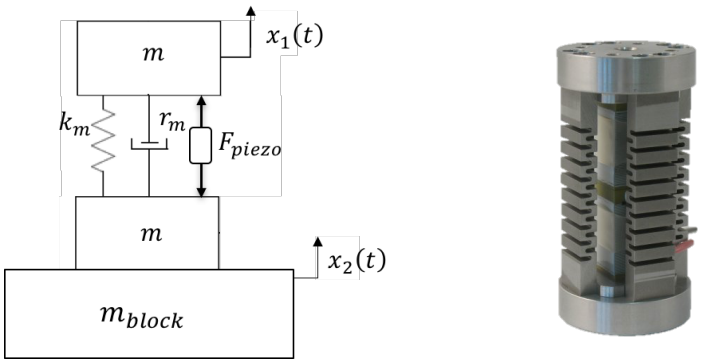

Figure 7: *2DOF Piezo/blocked model*

The parameters given in the Cedrat catalog were found to not reproduce our measurements precisely, so the parameters were tuned to match the experimental characterization of the piezo and validated using additional free – blocked case studies, as described below. Given a 2DOF system depicting the top of the piezo and the bottom of the piezo with a mass attached (m_{block}), the system transfer functions can be presented by the following equations of motion:

$$M\ddot{s} + C\dot{s} + Ks = F \tag{1}$$

$$M = \begin{bmatrix} m & 0 \\ 0 & m + m_{block} \end{bmatrix}, \quad C = \begin{bmatrix} r_m & -r_m \\ -r_m & r_m \end{bmatrix}$$
$$K = \begin{bmatrix} k_m & -k_m \\ -k_m & k_m \end{bmatrix}, \quad F = \begin{Bmatrix} F_{piezo} \\ -F_{piezo} \end{Bmatrix}, \quad s = \begin{Bmatrix} x_1 \\ x_2 \end{Bmatrix}$$

Given the input force of the piezo actuator, the transfer functions can be represented for each DOF by the following equations

$$H_1(\omega) = \frac{a}{V} = \frac{\omega^2 N}{2k_m + i2r_m\omega - m\omega^2} \tag{2}$$

$$H_2(\omega) = \frac{a}{V} = \frac{-\omega^2 N}{2k_m + i2r_m\omega - m\omega^2} \tag{3}$$

Table 5: *CEDRAT Piezo Model Parameters*

Parameters	**Catalog Values**	**Model Values**
$Mass\ (m)$	$0.0319\ kg$	$0.0319\ kg$
$Force\ Factor\ (N)$	39.14 N/V	39.14 N/V
$Resistance\ (r_m)$	136.11	136.11
$Stiffness\ (k_m)$	$155.08 N/\mu m$	$217.11 N/\mu m$
$Quality\ Factor\ (Q)$	20	20
$Resonance\ (w_r)$	$13600\ Hz$	$13600\ Hz$

To gauge the effectiveness of the model, using the above equations and the parameters in Table 1, the piezo electric model was evaluated against three case studies: (1) no blocked mass, (2) 0.34 kg block, and (3) 1.95 kg block. The values per the catalog were used in modeling the piezo actuator, with the exception of the axial stiffness of the piezo. Initially the curves showed a uniform offset, so the model stiffness was increased from the catalog value by 40% to bring the curves into agreement.

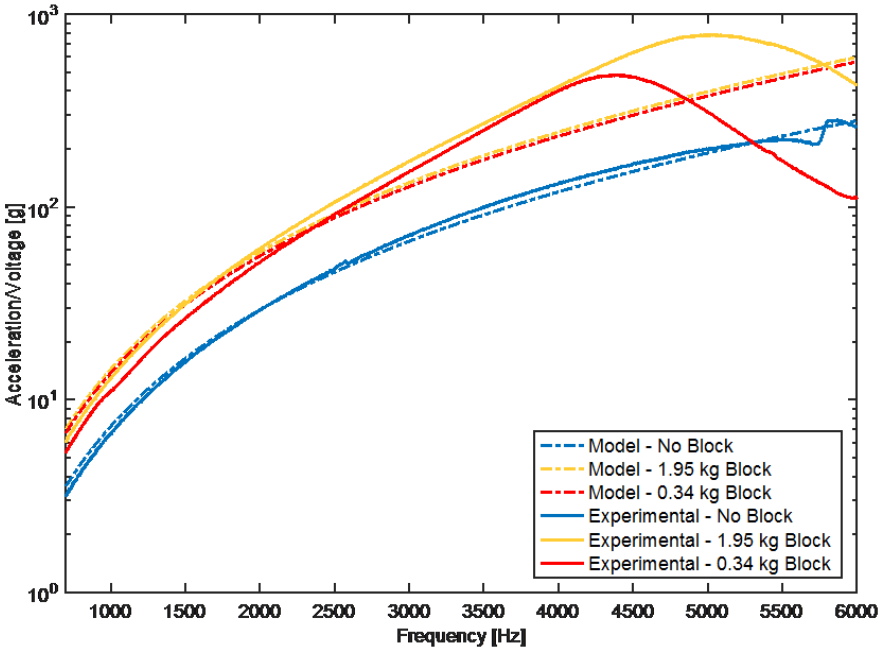

Figure 8: *Experimental vs. model results for motion at the top of the piezo actuator given an input voltage to the piezo actuator*

After these adjustments to the model parameters, the model now accurately reflects the acceleration transfer function up to about 2 kHz for all cases. At about 4-5 kHz the blocks exhibit a resonances that weren't included in the model, and so model can't be checked beyond that point. The measurements are all below the first elastic resonance of the piezo, which is nominally at 13.6kHz for the no block case, and so these measurements do not allow validating the stiffness rigorously. We presume that the model is sufficiently accurate to move forward.

4. COUPLED MODEL

The coupled component model features the conjunction of both models depicted in Section 2 and 3. The dynamics at the junction between the actuator and shaker are neglected to result in a 3DOF model given by: (1) Top of the piezo actuator, (2) junction between piezo and upper shaker armature, and (3) lower shaker armature as shown in Figure 9. Non-axial motion is not captured in this model.

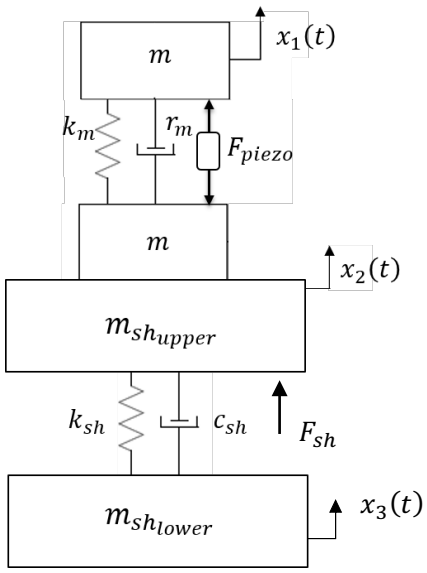

Figure 9: *3DOF model for the hybrid shaker – piezo system*

The 3DOF model maintains the parameters of the previous models and imposes the forcing of either the piezo, the shaker, or both on the model. The motion of the model hybrid system is governed by the following equation:

$$M\ddot{s} + C\dot{s} + Ks = F \tag{4}$$

$$M = \begin{bmatrix} m & 0 & 0 \\ 0 & m_{sh_{upper}} + m & 0 \\ 0 & 0 & m_{sh_{lower}} \end{bmatrix}, \quad C = \begin{bmatrix} r_m & -r_m & 0 \\ -r_m & r_m + c_{sh} & -c_{sh} \\ 0 & -c_{sh} & c_{sh} \end{bmatrix}$$

$$K = \begin{bmatrix} k_m & -k_m & 0 \\ -k_m & k_m + k_{sh} & -k_{sh} \\ 0 & -k_{sh} & k_{sh} \end{bmatrix}, \quad F = \begin{Bmatrix} F_{piezo} \\ -F_{piezo} + F_{sh} \\ 0 \end{Bmatrix}, \quad s = \begin{Bmatrix} x_1 \\ x_2 \\ x_3 \end{Bmatrix}$$

As a result, the model can then be compared to the experimental data of the piezo actuator on the shaker for two cases: (0) when the piezo was excited, and the shaker was off, and (1) when the piezo was off, and the shaker was excited. Any combination of the two cases can be used in union to result in a desired environment. In all cases, the acceleration at the top of the piezo was compared between experimental and model data to determine if the model captures the force transmissibility from the shaker to the piezo.

In the first case, the piezo was excited with a 200mV pseudorandom input. In essence, this is another blocked case for the piezo model, with the shaker providing the foundation. However, In the second case, the shaker was excited with a 50mV pseudorandom input. Unlike the piezo actuator, there is no empirical value for the force factor of the shaker. Given that the force of the shaker is unknown, the acceleration at the top of the plate and the armature mass was used to determine the force of the shaker using $F_{sh} = m_{sh}\ddot{x_2}$ where m_{sh} is the armature mass, assuming no energy loss between the joints connecting the plate to the shaker. The results of both cases are shown in Figure 10, comparing the model prediction to the experimental data at the top of the piezo actuator.

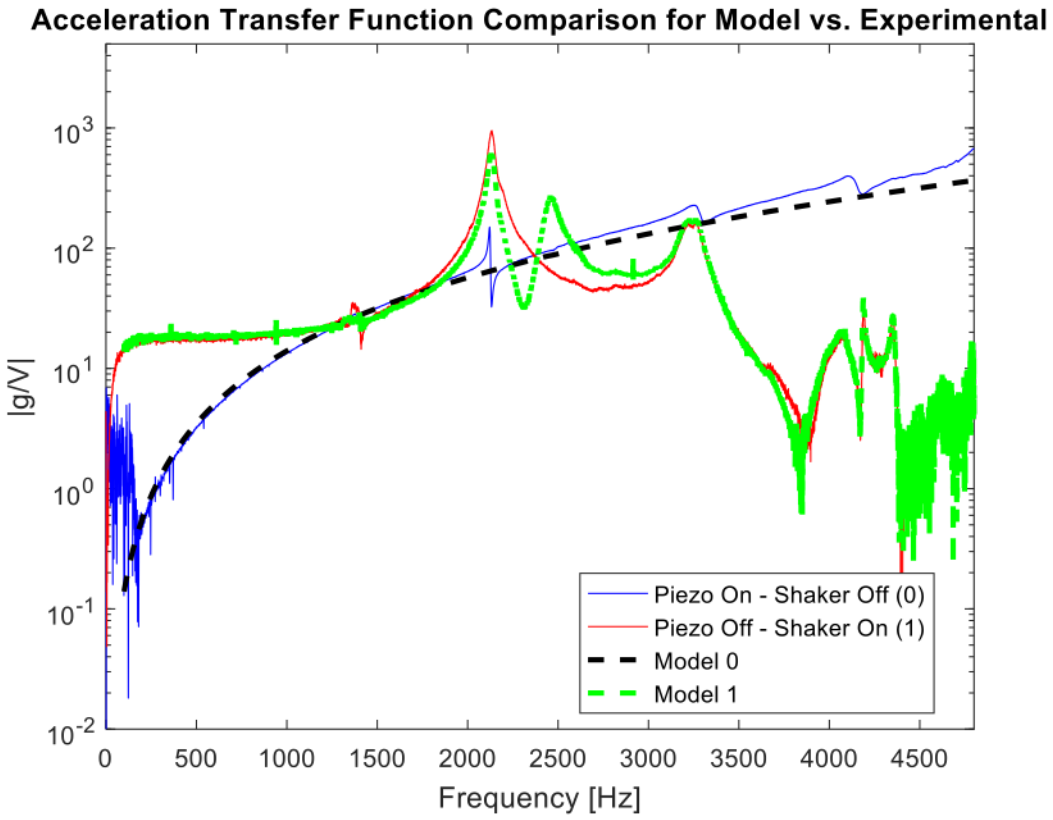

Figure 10: *3DOF model in comparison to the experimental acceleration data*

Within the range of interest, both models accurately capture the profile of the experimental data. Case one with the piezo actuator on and the shaker off is very accurately replicated by the model (recall that the stiffness factor for the piezo was scaled from the catalog value by 40% when tuning in the prior section). However, as expected, it cannot capture the additional resonances of the shaker, at the top of the piezo actuator. On the other hand, Model 1 is found to replicate the results for the case where the shaker is energized and the piezo is off but introduces an additional resonance at 2400 Hz. This resonance is thought to come about due to dynamics of the mounting plate located at the interface between the piezo actuator and the shaker, which is not accounted for within the model. In any event, this confirms that these models are able to reproduce the force generating ability of the piezo actuator and shaker, and hence they can now be used to determine what environments this combination of actuators can produce.

The second purpose for creating these models was to predict the stress in the piezo actuator to assure that it would not be damaged in the environments of interest. To do this, the strain of the piezo actuator in both cases was evaluated against experimental measurements. The displacements of the two masses in the piezo model were used to calculate the strain, which was then compared with measurements from a strain gauge mounted on the piezo as depicted below in Figure 11.

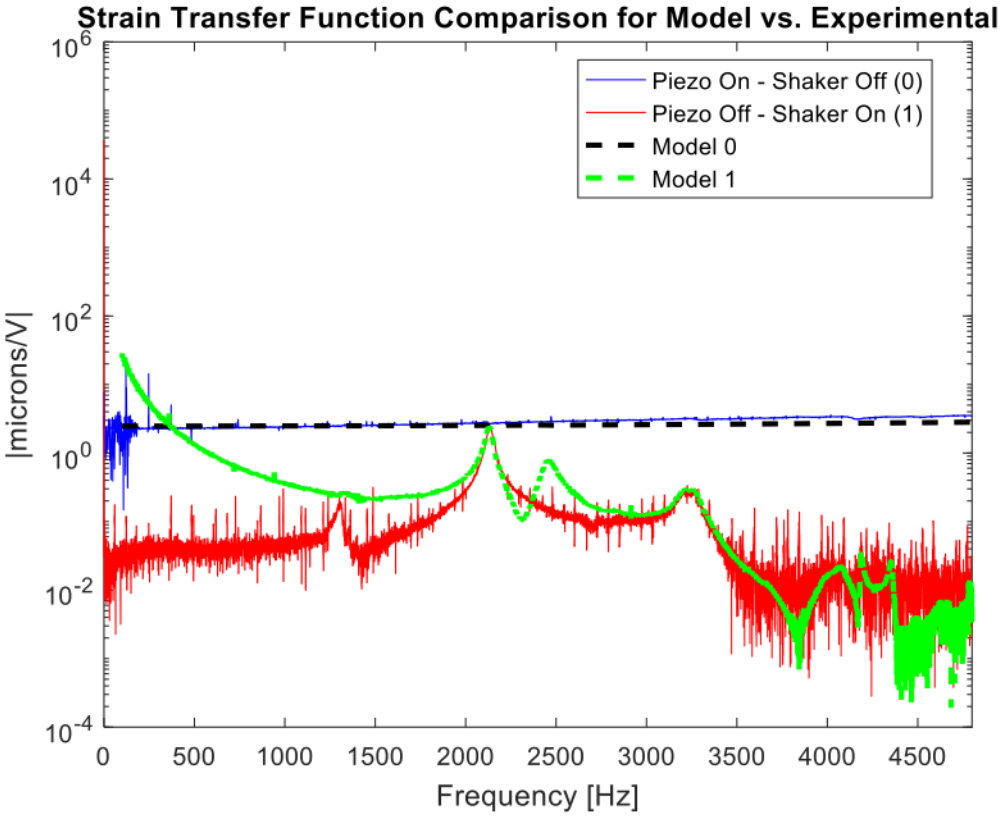

Figure 11: *3DOF model in comparison to the experimental strain data of the piezo actuator*

As with the acceleration FRFs, both models accurately reflect the experimental strain of the piezo actuator. Model 0 simply shows that the strain magnitude achieved by the piezo matches that predicted by the model and both are essentially static in the frequency range of interest. Model 1 (piezo off/shaker on) captures the key resonance in the system at 2.146 kHz, showing excellent agreement near that mode, and since this is the primary mode of interest at the moment the model is judged successful. However, Model 1 shows an error that manifests itself as an over – prediction in the strain at low frequencies for which the cause is not yet known. These models have now been shown to reproduce the ability of the actuators to generate force and the strain in the piezo due to each actuator. However, we have not yet verified that superposition is valid for this configuration nor has the linearity of the system been verified. Further testing is underway in which both actuators are used simultaneously to see whether the response and strains predicted obey superposition when both the piezo actuator and shaker are active.

The purpose of the shaker/piezo actuator hybrid system is to excite a test article to a certain environment, while not exceeding the limitations in the test hardware. An effective method to evaluate the effectiveness of this system is to estimate the voltage required to excite the test article to a certain acceleration and calculate the effective strain of the piezo actuator, such that it does not exceed hardware strain limitations. Assuming a desired ~8g rms environment, the model reveals that approximately 10V must be supplied to the shaker to create this environment for the desired frequency range (0 Hz – 4kHz) as detailed in the equations below:

$$rms\left(V_0 * H_a\left[\frac{g}{V}\right]\right) = a_{desired} \tag{5}$$

Where V_0 is the required voltage to produce the desired acceleration ($a_{desired}$) using the experimental FRF data. Likewise, the maximum effective strain of the piezo actuator can be found in a similar manner by using the voltage obtained in Equation 5 to evaluate the max strain in Equation 6.

$$\varepsilon_{max} = max\left(V_0 * H_{strain}\left[\frac{\mu m}{V}\right]\right) \quad (6)$$

Using this methodology, the maximum strain given a desired acceleration of 8g rms, for both cases is evaluated. For the first case with the shaker off and the piezo on, the maximum strain produced within the piezo is 12 microns, whereas for the second case with the shaker on and the piezo off, the maximum strain produced within the piezo is 45 microns. This is summarized in the table below.

Table 6: *Max piezo strain to produce a desired environment*

	Case 0 (Piezo on, shaker off)	**Case 1 (Piezo off, shaker on)**
Environment	8g rms	8g rms
Voltage Required	6.16 V	9.96 V
Max Piezo Strain	12.431 microns	45.009 microns

As evident, the second case exceeds the maximum strain allowed within the piezo of 44 microns [5]. Furthermore, even though the first case remains within the strain limitations of the piezo actuator, the voltage required exceeds the piezo limitations. The piezo itself is limited to 85 V, but the 20x multiplicity of the amplifier with the 6.16 V to the amplifier well exceeds this limitation. Hence, moving forward it will be necessary to limit each actuator to a subset of the frequency band (i.e. use the shaker from 0-3kHz and the piezo actuator from 3-5 kHz) in order to hopefully keep within the limitations of the piezo.

4.0 CONCLUSION

This work has explored the characterization of an electromagnetic shaker and piezoelectric actuator to create a hybrid system that could hopefully allow more faithful reconstruction of high frequency vibration environments. Tests were performed on each of the structures to establish low-order models and to understand what frequency range each model might be valid for. The models were then combined to create a model for the hybrid piezo/shaker system, and the resulting model was found to properly replicate the experimental data with the piezo actuator forcing the system and the shaker off, or with the actuator off and the shaker on. However, the measurements did show additional resonances that were not captured by the model, presumably due to additional modes in the experimental data. So far these modes are not dominant contributors to the environment or strain in the piezo, so they have been ignored but they certainly could be included in future models.

Future work will seek to validate the model with a superposition of forces to better correlate test cases where both the shaker and the piezo actuator are exciting the system. With the validation of the model, control schemes will be explored to evaluate the effectiveness in the mitigation of shaker anti-resonances and the ability to produce desired test environments through a closed loop configuration coupled with a vibration controller.

Works Cited

[1] W. J. DeLima and M. N. Ambrose, "Experimental Characterization And Simulation Of Vibration Environmental TesT," Kansas City, in Topic in Modal Analysis, vol 10, Chapter 6,Proceedingd pg *33rd IMAC - Conference & Exposition on Structural Dynamics* 2015.

[2] R. Jepsen and E. Romero, "Testing in a Combined Vibration and Acceleration Environment," in *IMAC - XXIII Conference & Exposition on Structural Dynamics*, 2005.

[3] M. S. Allen and J. H. Ginsberg, "A global, SIMO implementation of the algorithm of mode isolation and application to analytical and experimental data," *Mechanical Systems and Signal Processing,* vol. 20, no. 5, pp. 1090-1111, 2006.

[4] S. Waimer, S. Manzato, B. Peeters, M. Wagner and P. Guillaume, "A Multiphysical Modelling Approach for Virtual Shaker Testing Correlated with Experimental Test Results," in *Conference Proceedings of the Society for Experimental Mechanics Series*, 2016.

[5] CEDRAT TECHNOLOGIES, "Products Catalog," 2016.